XX IMEKO World Congress
Metrology for Green Growth
September 9–14, 2012, Busan, Republic of Korea

DETERMINATION OF THE DISTORTION COEFFICIENT OF A 500 MPA FREE-DEFORMATION PISTON GAUGE USING A CONTROLLED-CLEARANCE ONE UP TO 200 MPA

Yuanchao Yang, Jin Yue

National Institute of Metrology (NIM), Beijing 100013, China
Email: yangyc@nim.ac.cn

Abstract: Cross-float experiments between a 500 MPa free-deformation (FD) piston gauge and a 200 MPa controlled-clearance (CC) one were carried out at a series of system pressures and jacket pressures. The two characteristics of the CC piston gauge, the zero clearance jacket pressure and the jacket pressure coefficient, were determined based on the Heydemann-Welch model. After that, the pressure dependence of the effective area for the FD piston was calculated using the cross-float data, from which the pressure distortion coefficient was determined to be 8.46×10^{-7} MPa^{-1}. The result was about 19% larger than the one obtained by the Lame equation.

Keywords: distortion coefficient; controlled-clearance piston gauge; Heydemann-Welch model; effective area; cross-float experiment.

1. INTRODUCTION

The pressure scale at the National Institute of Metrology (NIM) is up to 500 MPa, which is realized by a free-deformation (FD) piston gauge of 5 MPa/kg made by DH Instruments, USA[1], referred to as FD500. The uncertainty of its effective area due to the distortion becomes more significant in this pressure range, especially above 100 MPa. To obtain adequate small uncertainty in the pressure region of 500 MPa, the key point is to accurately determine the distortion coefficient of FD500. Generally, the distortion coefficient can be evaluated by theory or experiment. In theory, the methods include simple calculations based on the Lame equation and finite elemental analysis (FEA) [1-4]. The theoretical calculations need good knowledge of the elastic constants and the piston-cylinder dimensions, the boundary loading conditions and the fluid properties. With the elastic constants unknown and using literature values, the calculation based on the Lame equation could result a disagreement of 20% [5]. Large disagreement also revealed when using the FEA method [6]. In experiment, the distortion coefficient can be obtained by the similarity method [7] or calibrating against a well characterized piston gauge. The controlled-clearance (CC) piston gauge is widely used as a primary pressure standard above 100 MPa [8, 9], of which the distortion coefficient can be well characterized by an independent experiment using the Heydemann-Welch (HW) method [10-12].

In this paper, cross-float experiments were performed between the FD500 and a 200 MPa CC piston gauge of 2 MPa/kg, which is also made by DH Instrument[1] and denoted as CC200. On one hand, the CC200 was characterized using the HW model. Its pressure dependence of the effective area and uncertainty were evaluated. On the other hand, the pressure dependence of the effective area for FD500 was also obtained in the pressure range of 200 MPa.

2. PRINCIPLE AND EXPERIMENTAL SETUP

The FD500 and CC200 were connected to the pressure line with valves and a digital pressure monitor gauge. Another free-deformation piston gauge of 100 MPa was used to apply the jacket pressure. The pressure-transmitting fluid in both lines was Di(2-ehtylhexyl) sebacate.

In the HW model, the effective area of the CC piston gauge is expressed as

$$A_{e,CC} = A_{0,T_0}[1+(\alpha_p+\alpha_c)(T-T_0)](1+bp_s)[1+d(p_z-p_j)] \quad (1)$$

where $A_{0,T0}$ is the piston area at zero pressure and the reference temperature, p_s is the system pressure, b is the distortion coefficient of the piston, α_p and α_c are the thermal expansion coefficients of the piston and cylinder, T is the temperature of the piston-cylinder and T_0 the reference temperature (20 ℃), p_j is the jacket pressure. The jacket pressure coefficient d and the zero clearance jacket pressure p_z are two modelling parameters.

The jacket pressure coefficient d is the relative change in the effective area in response to the jacket pressure and can be determined as

[1] Certain commercial equipment, instruments or materials are indentified in this paper to foster understanding. Such identification does not imply endorsement by the authors nor dose it imply that the equipment or materials are necessarily the best for the purpose.

$$d = -\frac{1}{\Delta p_j}\left(\frac{\Delta A_e}{A_e}\right) \approx \left|\frac{1}{\Delta p_j}\left(\frac{\Delta M}{M}\right)\right| \quad (2)$$

where ΔA_e and ΔM are the change in the effective area of CC piston gauge and the change in mass to achieve new equilibrium under Δp_j.

The zero clearance jacket pressure p_z means the jacket pressure at which the clearance between the piston and cylinder vanishes, and the piston fall-rate turns 0. Under laminar-flow conditions, the cubic root of the piston fall-rate v is proportional to the piston-cylinder clearance h, which is also proportional to (p_z-p_j). Consequently, the relationship between p_j and v can be written as

$$p_j = kv^{1/3} + p_z \quad (3)$$

where k is a constant depending on p_s. The zero clearance jacket pressure p_z is determined by measuring the piston fall-rate v under different p_j and extrapolating the plot of p_j versus $v^{1/3}$ to $v^{1/3}$=0. The piston fall-rate was measured by a built-in linear variable differential transformer (LVDT), which was calibrated using a cathetometer. The piston position was recorded using a computer through the remote communication port over 3 min to 8 min, and the fall-rate was calculated from the linear fit of the position versus time data. To eliminate the temperature effect, all the fall-rate data were corrected for the temperature dependence of the viscosity of the pressure fluid [13].

The cross-float and fall-rate measurements were carried out at system pressures p_s from 40 MPa to 200 MPa in steps of 20 MPa. At each p_s, the jacket pressure p_j was initially set as 0, and then varied from 10% to 50% of p_s in steps of 4 MPa.

3. RESULTS OF THE EXPERIMENTS

3.1 Characterization of CC200

3.1.1 Zero clearance jacket pressure p_z

Fig. 1 shows the results of piston fall-rate measurements, and p_j is plotted against $v^{1/3}$ at each system pressure. According to equation (3), the experimental data are fitted to linear functions (solid lines in Fig. 1), and p_z is estimated by the intercept on y-axis of the fitted line. At p_s above 100 MPa, the linear fits show some deviations from the experimental data at p_j=0 and upper limits of p_j.

The determined p_z is plotted against p_s, as shown in Fig. 2, and a quadratic polynomial is fitted to the data giving

$$p_z = 107.55 + 0.3138\,p_s + 8.097\times10^{-4}\,p_s^{\,2} \quad (4)$$

The value of p_z predicted by equation (4) is used in the HW model, with the uncertainty estimated by the combination of the one originated from the fit of p_j versus $v^{1/3}$ and the one from the fit of p_z versus p_s. The values of p_z at each system pressure with their uncertainties are summarized in Table 1.

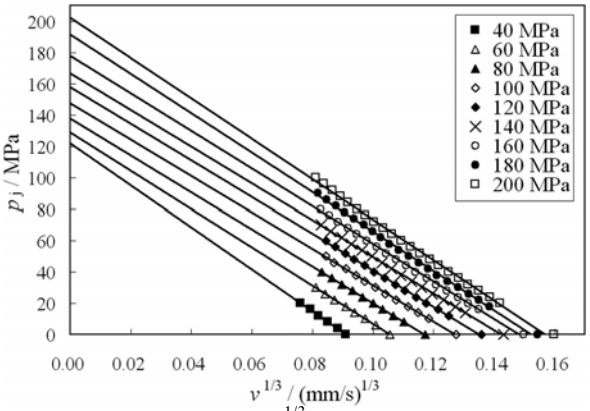

Fig. 1. Plot of p_j against $v^{1/3}$ at system pressures from 40 MPa to 200 MPa. Solid lines represent the linear fits to the data.

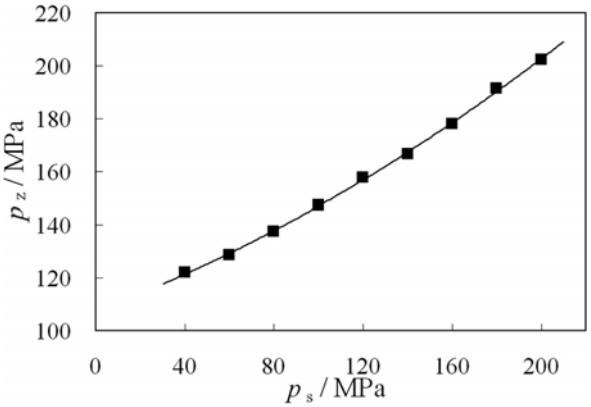

Fig. 2. Zero clearance jacket pressure p_z as a quadratic function of system pressure p_s.

3.1.2 Jacket pressure coefficient d

To determine the jacket pressure coefficient d, cross-float experiments were performed between CC200 and FD500 at different jacket pressure p_j. With p_j increased, the effective area of CC200 was decreased and the mass added on CC200 was reduced. Comparing to the effective area of CC200 at zero jacket pressure, the relative change in effective area at p_j, $-\Delta A_e / A_e$, was calculated based on the relative change in mass taking account of the correction for the buoyancy and temperature effect. As an example, Fig. 3 shows the plot of the relative change in effective area versus p_j at the system pressure of 200 MPa. Applying linear fit to the data, d is derived from the slope of the fitted straight line. However, Fig. 3 also reveals deviation from the linear fit. As a linear function of p_j, the behavior of the relative change in effective area at very low p_j is different from that at very high p_j, implying a p_j dependence of d. The nonlinearity appears at p_s above 120 MPa, while the data keep good linearity at p_s of 120 MPa and below. The nonlinear behavior in the plot of $-\Delta A_e / A_e$ versus p_j at higher p_s is coherent with the nonlinearity in the plot of p_j versus $v^{1/3}$ mentioned above. The influence of nonlinearity on the value of p_z and d is considered as an uncertainty component, and will be discussed in Section 3.1.4.

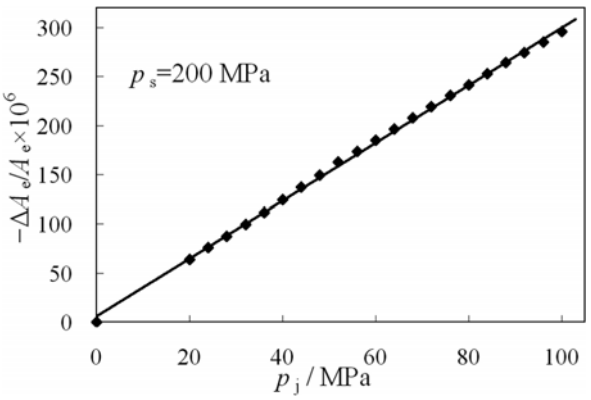

Fig. 3. Relative change in effective area as a linear function of p_j at p_s=200 MPa.

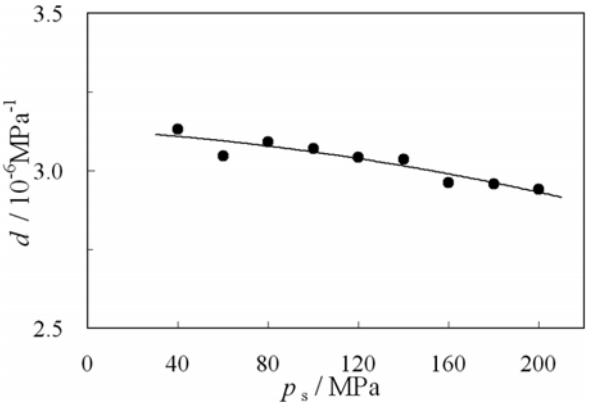

Fig. 4. Plot of d against p_s. Solid line is the quadratic fit to the data.

The jacket pressure coefficient d obtained at each system pressure is plotted against p_s, as shown in Fig. 4. Fitting to a quadratic function, d can be expressed as

$$d = (3.130 - 4.19\times10^{-4}\, p_s - 2.86\times10^{-6}\, p_s^{\,2})\times10^{-6} \quad (5)$$

The uncertainty of the fitted d is the combination of the one originated from the fit of $-\Delta A_e / A_e$ against p_j and the one from the fit of d against p_s. The fitted values of d and their uncertainties are listed in Table 1.

Table 1. Fitted values of p_z, d and their standard uncertainties.

p_s MPa	p_z MPa	$u(p_z)$ MPa	d $\times10^{-6}$ MPa^{-1}	$u(d)$ $\times10^{-6}$ MPa^{-1}
40	121.40	1.92	3.109	0.033
60	129.30	1.16	3.094	0.056
80	137.84	0.49	3.078	0.017
100	147.03	1.01	3.059	0.015
120	156.87	1.39	3.038	0.009
140	167.36	1.11	3.015	0.024
160	178.49	1.30	2.990	0.030
180	190.27	1.72	2.962	0.016
200	202.70	1.74	2.932	0.022

3.1.3 Piston distortion coefficient b

The piston distortion coefficient b is calculated from the elastic theory as

$$b = (3\sigma - 1)/E \quad (6)$$

where σ and E are Poisson's ratio and Young's modulus of the material, respectively. The piston is made from tungsten carbide. With σ of 0.218 and E of 560 GPa provided by the manufacturer, b is obtained as -6.18×10^{-7} MPa^{-1}. The semi-range of b is evaluated as 10% and assuming a uniform distribution. The standard uncertainty of b is taken as $u(b)$=3.57×10^{-8} MPa^{-1}.

3.1.4 Pressure dependence of the effective area of CC200

After the determination of p_z, d and b, the pressure dependence of the effective area of CC200 is characterized according to equation (1) as

$$C_p = (1 + bp_s)[1 + d(p_z - p_j)] \quad (7)$$

Fig. 5 shows the plot of C_p against p_s at jacket pressure of 0%, 25% and 50%, respectively. The error bars represent the standard uncertainty of C_p. It can be seen that the distortion coefficient is almost zero when the jacket pressure is applied as 25% p_s.

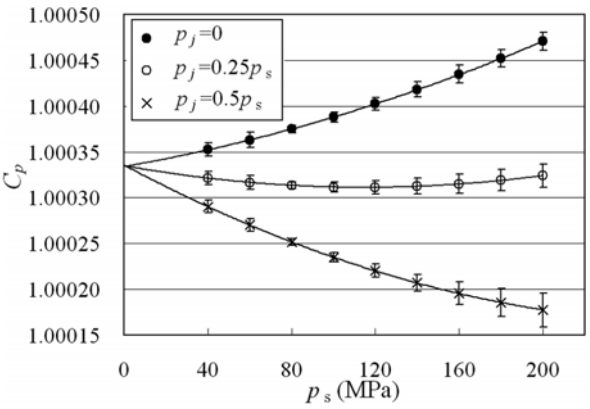

Fig. 5. Pressure dependence of the effective area of CC200 at p_j=0, 0.25 p_s, and 0.5 p_s, respectively.

The uncertainty of C_p is considered to have two components. One component, $u_1(C_p)$, is the root sum square of $u(b)$ p_s, $u(d)$ (p_z- p_j), and $u(p_z)d$. The other component, $u_2(C_p)$, is derived from the nonlinearity in the determination of p_z and d observed at higher system pressure. Because of the nonlinearity, the p_z and d value is dependent on the selected range of the linear fit. If the data at higher p_j were used, p_z would be overestimated and d underestimated. Conversely, p_z would be underestimated and d overestimated if data at lower p_j were used. The influence of the selected range on p_z and d is correlated, and their effects on C_p are cancelled partly. To calculate $u_2(C_p)$, p_z and d at p_s above 100 MPa are redetermined by linear fitting to the data at higher p_j, and new result of C_p is obtained. The difference between the new result of C_p and the original value is taken as $u_2(C_p)$. At p_j=0, 0.25 p_s, and 0.5 p_s, the two uncertainty components $u_1(C_p)$, $u_2(C_p)$ and the combined uncertainty $u(C_p)$ are summarized in Table 2.

Table 2. Uncertainty of C_p in the case of p_j=0, 0.25 p_s, and 0.5 p_s.

	p_j=0			p_j=0.25 p_s			p_j=0.5 p_s		
p_s MPa	u_1	u_2	u	u_1	u_2	u	u_1	u_2	u
					10^{-6}				
40	7.3	0.1	7.3	7.1	0.1	7.1	7.0	0.2	7.0
60	8.4	0.1	8.4	7.7	0.0	7.7	7.0	0.0	7.0
80	4.0	0.8	4.1	3.8	0.6	3.8	3.6	0.5	3.7
100	5.2	1.9	5.5	5.1	1.8	5.4	4.9	1.8	5.3
120	6.2	3.1	6.9	6.1	3.5	7.0	6.1	3.8	7.2
140	7.2	4.1	8.3	6.8	5.3	8.6	6.4	6.5	9.2
160	8.8	4.3	9.8	8.1	7.0	11	7.5	9.6	12
180	8.8	3.3	9.4	8.5	8.1	12	8.4	13	15
200	9.8	0.6	9.8	9.4	8.3	13	9.1	16	18

The uncertainty component $u_1(C_p)$, due to p_z, d and b, is similar in all the case of p_j. The uncertainty $u_2(C_p)$ due to the nonlinearity is very small when the jacket pressure is 0. However, at higher p_j, $u_2(C_p)$ becomes dominant when p_s is above 100 MPa. As a result, the combined uncertainty of C_p at higher p_j and higher p_s is significantly larger than that in the case of p_j=0. Since the uncertainty is relatively small at p_j=0, the piston gauge CC200 described here is recommended to be used with zero jacket pressure.

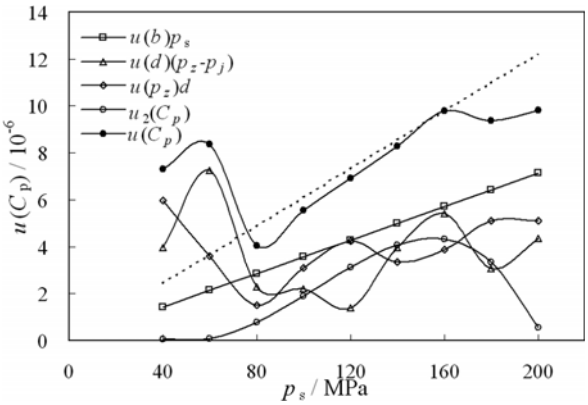

Fig. 6. Plot of the uncertainty of C_p and its components as a function of system pressure.

In the case of p_j=0, the uncertainty components and the combined uncertainty of C_p are plotted as a function of p_s, as shown in Fig. 6. For CC200 used with p_j=0, the uncertainty due to the pressure dependence of the effective area is less than 6.2×10^{-8} MPa^{-1} at p_s of 80 MPa and above. However, when CC200 is used with p_j=0.5p_s, this value would be 9.2×10^{-8} MPa^{-1}.

3.1.5 Piston area $A_{0,T0}$

At p_j=0, CC200 was calibrated against a 100 MPa FD pressure standard, of which the effective area was traceable to the NIM primary pressure standard of 10 MPa [14]. Details of the traceability will be presented elsewhere. From the calibration, the piston area $A_{0,T0}$ was determined to be 4.902162 mm^2 with a relative standard uncertainty of 1.7×10^{-5}.

3.2 Characterization of FD500

Based on the characterization of CC200, the cross-float data used to determine d were used again to calculate the effective area of FD500 at each p_s. Using the result at p_j=0, the effective area A_p is plotted against p_s, as shown in Fig. 7. The effective area is modelled by a linear function of p_s as

$$A_p = A_0(1+\lambda p_s) \tag{8}$$

where A_0 is the zero-pressure effective area and λ is the distortion coefficient. A linear fit to the data gives the results of A_0, λ and their standard deviations as

$$A_0 = 1.962244 \text{ mm}^2 \quad s_r(A_0) = 8.1\times10^{-6}$$
$$\lambda = 8.46\times10^{-7} \text{ MPa}^{-1} \quad s(\lambda) = 6.2\times10^{-8} \text{ MPa}^{-1} \tag{9}$$

where $s_r(A_0)$ is the relative standard deviation of A_0 and $s(\lambda)$ is the standard deviation of λ. Taking into account the uncertainty due to the parameters of CC200, which are discussed in Section 3.1.4 and 3.1.5, the combined uncertainty of A_0 and λ are estimated as

$$u_r(A_0) = 1.9\times10^{-5}$$
$$u(\lambda) = 8.8\times10^{-8} \text{ MPa}^{-1} \tag{10}$$

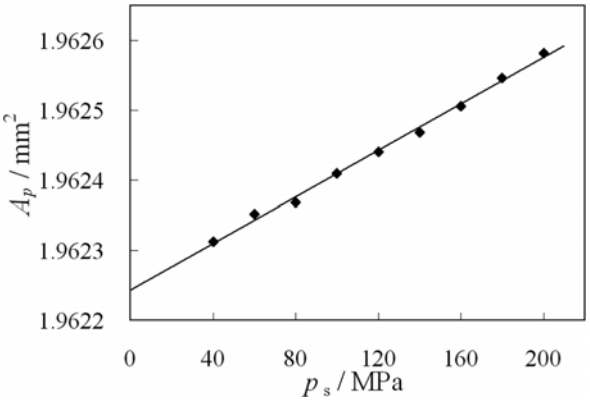

Fig. 7. Pressure dependence of the effective area of FD500 from 40 MPa to 200 MPa. The result is obtained at p_j=0.

Fig. 7 shows good linearity, and the deviation from the linear fit is found to be less than $\pm5\times10^{-6}$. Strictly speaking, the determined distortion coefficient is only valid in the pressure range of 200 MPa, which is only 40% of the full scale of FD500. However, we assumed the linearity could be extended up to 500 MPa. The assumption is reasonable, since the deviation from the linearity for a similar piston gauge has been reported to be less than $\pm5\times10^{-6}$ in the full scale of 500 MPa [12].

4. DISCUSSION

The effective area and distortion coefficient of FD500 described here are traceable to the NIM primary standard and CC200, respectively. The distortion coefficient was determined experimentally using a CC piston gauge based on the HW method. On the theory point of view, the distortion coefficient can be calculated based on the elastic theory with the information of the material properties. For simple FD

piston gauge, a simplified calculation based on the Lame equation is expressed as

$$\lambda = \frac{3\sigma_p - 1}{2E_p} + \frac{1}{2E_c}\left(\frac{R_c^2 + R_p^2}{R_c^2 - R_p^2} + \sigma_c\right) \quad (11)$$

where σ_p, σ_c is the Poisson's ratio of piston and cylinder, E_p, E_c is the Young's modulus of piston and cylinder, R_p is the radius of piston or the inner radius of cylinder, R_c is the outer radius of cylinder. In the case of FD500, the piston and cylinder all are made from tungsten carbide, the Poisson's ratio and Young's modulus for piston are 0.218, 560 GPa, and 0.218, 620 GPa for cylinder provided by the manufacturer. R_p and R_c are measured to be 0.79 mm and 10 mm, respectively. Using these data and equation (11), the distortion coefficient is calculated to be 6.83×10^{-7} MPa^{-1}. Taking the uncertainty of Poisson's ratio and Young's modulus as 0.01 and 50 GPa, the uncertainty of the calculated distortion coefficient is estimated to be 8.9×10^{-8} MPa^{-1}. Comparing to the value determined by experiment, which is 8.46×10^{-7} MPa^{-1} with an uncertainty of 8.8×10^{-8} MPa^{-1}, the two results are badly consistent. The difference between the two results is 1.63×10^{-7} MPa^{-1}, about 19% of the experimental value, and can cause a relative deviation of 8.2×10^{-5} in effective area at 500 MPa. The distortion coefficient calculated here is unreliable, because equation (11) is an approximation under ideal conditions and the elastic parameters are not measured directly. It may improve the theoretical result by applying FEA to the real structure of the piston-cylinder unit and using more accurate elastic parameters.

Using experimental method to determine the distortion coefficient, the nonlinearity of the CC piston gauge at high system pressure is a problem. This problem may be solved using a higher order HW model. However, it needs to extend the jacket pressure range to much higher region close to the zero clearance jacket pressure, and that may damage the piston and it's difficult to measure the extremely slow fall-rate.

5. CONCLUSIONS

The distortion coefficient of FD500 was studied using CC200 based on the HW method. Piston fall-rate measurements and cross-float experiments were carried out at jacket pressures from 0 to 50% of system pressure. Nonlinearity was observed at system pressure above 100 MPa. The uncertainty of the pressure dependence of the effective area of CC200 was found to be smallest in the case of p_j=0 than in other case. Using the cross-float data at p_j=0, the distortion coefficient of FD500 was determined to be 8.46×10^{-7} MPa^{-1} with an uncertainty of 8.8×10^{-8} MPa^{-1}. The result is about 19% larger than the one obtained from the simply calculation based on the Lame equation. The extraordinary discrepancy may arise from the oversimplified calculation and inaccurate elastic parameters. In order to improve the consistency between the results of experiment and theory, future work will focus on FEA and measurements of material properties.

REFERENCES

[1] G. Buonanno, M. Dell'Isola, G. Iagulli and G. Molinar, "A Finite Element Method to Evaluate the Pressure Distortion Coefficient in Pressure Balances," High Temp.—High pressures, vol. 31, pp. 131-143, 1999.

[2] G. Molinar, G. Buonanno, G. Giovinco, P. Delajoud and R. Haines, "Effectiveness of Finite Element Calculation Methods (FEM) on High Performance Pressure Balances in Liquid Media up to 200 MPa," Metrologia, vol. 42, pp. S207-S211, 2005.

[3] W. Sabuga, G. Molinar, G. Buonanno, T. Esward, J. C. Legras and L. Yagmur, "Finite Element Method Used for Calculation of the Distortion Coefficient and Associated Uncertainty of a PTB 1 GPa Pressure Balance—EUROMET Project 463," Metrologia, vol. 43, pp. 311-325, 2006.

[4] S. Dogra, S. Yadav and A. K. Bandyopadhyay, "Computer Simulation of a 1.0 GPa Piston-Cylinder Assembly Using Finite Element Analysis (FEA)," Measurement, vol. 43, pp. 1345-1354, 2010.

[5] G. F. Molinar, "An Old Instrument in the New Technological Scenery: The Piston Gauge in Liquid Media up to 1 GPa," Metrologia, vol. 30, pp. 615-623, 1993/94.

[6] M. P. Fitzgerald and C. M. Sutton, "Pressure Balance Elastic Distortion: Experiment versus Theory," Metrologia, vol. 42, pp. S239-S241, 2005.

[7] R. S. Dadson, R. G. P. Greig and A. Horner, "Developments in the Accurate Measurement of High Pressures," Metrologia, vol. 1, pp. 55-67, 1965.

[8] A. K. Bandyopadhyay and A. C. Gupta, "Realization of a National Practical Pressure Scale for Pressures up to 500 MPa," Metrologia, vol. 36, pp. 681-688, 1999.

[9] J. K. L. Man, "Establishment of an Australian High Pressure Standard," Metrologia, vol. 42, pp. S169-S172, 2005.

[10] P. L. M. Heydemann and B. E. Welch, Experimental Thermodynamics. London: International Union of Pure and Applied Chemistry, Ch. 4, pp. 147-202, 1975.

[11] A. K. Bandyopadhyay and D. A. Olson, "Characterization of a Compact 200 MPa Controlled Clearance Piston Gauge as a Primary Pressure Standard using the Heydemann and Welch Method," Metrologia, vol. 43, pp. 573-582, 2006.

[12] H. Kajikawa, K. Ide and T. Kobata, "Precise Determination of the Pressure Distortion Coefficient of New Controlled-Clearance Piston-Cylinders based on the Heydemann-Welch Model," Rev. Sci. Instum., vol. 80, no. 9, pp. 095101 1-10, Sept. 2009.

[13] P. Vergne, "New High-pressure Viscosity Measurements on Di(2-ethylhexyl) Sebacate and Comparisons with Previous Data," High Temp.—High pressures, vol. 22, pp. 613-621, 1990.

[14] Y. C. Yang and J. Yue, "Calculation of Effective Area for the NIM Primary Pressure Standards," PTB-Mitteilungen, vol. 121, pp. 266-269, 2011.